HAL
open science

Evolution of dolomite composition and reactivity during biomass gasification

Maxime Hervy, Roberto Olcese, Mohammed Bettahar, Martine Mallet, Aurélien Renard, Libeth Maldonado, Damien Remy, Guillain Mauviel, Anthony Dufour

To cite this version:

Maxime Hervy, Roberto Olcese, Mohammed Bettahar, Martine Mallet, Aurélien Renard, et al.. Evolution of dolomite composition and reactivity during biomass gasification. Applied Catalysis A : General, 2019, 572, pp.97-106. 10.1016/j.apcata.2018.12.014 . hal-01969516

HAL Id: hal-01969516

https://hal.univ-lorraine.fr/hal-01969516

Submitted on 12 Oct 2021

HAL is a multi-disciplinary open access archive for the deposit and dissemination of scientific research documents, whether they are published or not. The documents may come from teaching and research institutions in France or abroad, or from public or private research centers.

L'archive ouverte pluridisciplinaire **HAL**, est destinée au dépôt et à la diffusion de documents scientifiques de niveau recherche, publiés ou non, émanant des établissements d'enseignement et de recherche français ou étrangers, des laboratoires publics ou privés.

Version of Record: https://www.sciencedirect.com/science/article/pii/S0926860X18306100
Manuscript_70b42ed58d986b3ed0f80c367c4928f2

Evolution of dolomite composition and reactivity during biomass gasification

Maxime Hervy[a], Roberto Olcese[a], Mohammed M Bettahar[b], Martine Mallet[c], Aurélien Renard[c], Libeth Maldonado[a], Damien Remy[a], Guillain Mauviel[a], Anthony Dufour[a,*]

[a] LRGP, Université de Lorraine, CNRS, ENSIC, 1, Rue Grandville 54000 Nancy, France
[b] Institut Jean Barriol, L2CM, Université de Lorraine, CNRS, Faculté des Sciences et de la Technologie Boulevard des Aiguillettes, BP 7036, 54506 Vandœuvre Cedex, France
[c] Institut Jean Barriol, LCPME, Université de Lorraine, CNRS, 405, rue de Vandoeuvre, F-54600 Villers-lès-Nancy, France

* corresponding author at: anthony.dufour@univ-lorraine.fr

Abstract

Dolomite is a cheap and robust catalyst used for biomass gasification, but its deactivation under relevant conditions of pilot-scale gasifiers has still been poorly understood. For this reason, the catalytic activity of fresh and used dolomites produced from an industrial air-blow fluidized bed was investigated. Fresh and used dolomites were characterized by BET, SEM-EDX, XPS, ICP-MS, XRD, TPD and TPO. Benzene steam reforming was selected as a surrogate reaction of tar conversion in order to probe the reactivity of the two dolomites. The activity of used dolomite was 25% lower than that of fresh dolomite. This difference could be explained by: (1) the deposition of a Si-based layer from biomass ashes at the surface of used dolomite, and (2) the production of coke during gasification. The reaction mechanism of benzene steam reforming over fresh and used dolomites was discussed. For used dolomite, the Si and coke depositions reduced the availability of the active sites (CaO, MgO) thus lowering the conversion of benzene. These deposits could also inhibit the interactions between CaO and MgO and enhance the formation of a stable coke.

© 2018 published by Elsevier. This manuscript is made available under the CC BY NC user license
https://creativecommons.org/licenses/by-nc/4.0/

Keywords

biomass; dolomite; gasification; syngas; tar; up-grading.

Outline (only for reviewers)

1. Introduction **3**

2. Materials & Methods **3**

2.1. Presentation of the dolomite samples 3

2.2. Characterizations of the catalysts 3

2.3. Catalytic experiments 3

3. Results and discussion **3**

3.1. Characterization of the catalysts 3

3.1.1. Morphology of particles and chemical composition of the bulk catalysts by ICP 3

3.1.2. XRD characterization of the catalysts 3

3.1.3. Composition of the surface by XPS 3

3.1.4. TPD and TPO characterizations 3

3.2. Steam reforming of benzene over fresh and used dolomites 3

3.3. Discussion on the reaction mechanisms 3

4. Conclusion **3**

1. Introduction

Renewable alternative routes for energy production appear as an important challenge to reduce the greenhouse gases emissions while meeting the growing world energy demand. Biomass gasification is an attractive way to convert a renewable resource into several energy carriers, such as substitute natural gas, bio-hydrogen, or Fischer-Tropsch biofuel [1]. Nevertheless, the removal of the syngas pollutants (such as tars) is required before further valorization, and this step remains the major issue in the development of gasification processes. Tar is formed by pyrolysis reactions combined with incomplete oxidation reactions in gasifiers [2–4] and is the most problematic pollutant contained in the syngas [2]. Tar is composed of a wide variety of aromatic and oxygenated compounds classified in different classes depending on their properties [5] or their thermal history (primary, secondary and tertiary tar) [2]. These compounds can condense along the process chain thus impeding syngas valorization. The concentration of tar must be drastically reduced in order to meet the standards required for syngas ranging from about 50 mg/Nm^3 (or a dew point lower than 35°C for engine [6]) to 0.1 mg/Nm^3 (for Fischer-Tropsch synthesis) [7]. In addition, tar in syngas considerably reduces the cold gas efficiency of gasifiers. Indeed, benzene can represent 0.5% of biomass LHV in air dense fluidized bed gasifier [3].

For these reasons, the catalytic conversion of tar into gaseous products (CO, H_2, CH_4) is of tremendous importance for improving the gasification processes. The main drawbacks of the catalytic methods are the cost of the catalysts and their deactivation. This topic has been intensively studied over the past 30 years, and several reviews have reported the main conclusions [8–20]. These studies focused on the conversion of real biomass tars, or tar surrogate molecules. Benzene, toluene and naphthalene are often considered as surrogate tar compounds due to their significant concentration in syngas and to their stability [9,21,22]. Benzene is the most important aromatic compound present in the syngas and the most stable one [22–24]. For this reason it is a good surrogate of tertiary (high temperature) tar.

A large variety of catalysts were tested for tar decomposition: chars [25–28], zeolites [29,30], iron oxides [31], noble metals [32–37], alkaline and alkaline earth metals (AAEM) [38,39], nickel catalysts [40,41], clay minerals [13], olivine [42,43], and calcined rocks (magnesite, calcite, dolomite) [44–46]. Carbonate rocks, such as dolomite, were identified as promising catalysts due their abundance and low-cost [47–51].

Dolomite is a natural magnesium ore ($MgCO_3.CaCO_3$) composed of a mixture of calcium carbonate and magnesium carbonate at a concentration ratio of nearly 1:1. A tremendous number of articles highlighted that dolomite is an active catalyst for tar removal [48,52–64]. A calcination

step is required to increase the catalytic activity of dolomite by eliminating CO_2 and transforming ($CaMg(CO_3)_2$) into active CaO and MgO [65]. CaO is known to be more active than MgO in tar cracking reactions and is mainly responsible for the high activity of calcined dolomite [66]. However, a synergistic interaction between CaO and MgO plays an important role in the activity of dolomite. Indeed, catalysts based on mechanical mixtures of MgO and CaO have presented a better performance than CaO alone [67]. In addition, dolomite was proved to be more active than magnesite ($MgCO_3$) and calcite ($CaCO_3$) for tar reforming [50,64]. The higher activity of dolomite is mainly explained by the lower deactivation by coke deposition, as a result of the presence of MgO which inhibits the formation of stable carbonaceous materials at the surface of CaO, and which promotes the formation of less stable carbon species that are easily gasified [68]. Therefore, the deactivation of CaO active sites by coke deposition is reduced. The presence of iron in dolomites is also expected to play a role in the steam reforming of tar as well as in the water-gas shift reaction [56,64].

Some articles specifically studied the decomposition of benzene [52,54], toluene [69–71] and naphthalene [53,72] over calcined dolomite. The tests were conducted at 700-900 °C under different atmospheres: steam, carbon dioxide or syngas mixtures. The benzene decomposition reactions mainly generated H_2 and CO_2, while CO was a minor product and was generated in lower amount with rising temperature. These reactions were inhibited by hydrogen which may be dissociatively adsorbed on the metal-oxide adsorption sites, thus preventing the tar access to adsorption sites [73,74]. The CO_2 concentration in the syngas and the temperature strongly influence the activity of dolomite. Indeed, the dolomite can be carbonated (depending on the thermodynamic equilibrium of $CO_2/CaO/CaCO_3$) which results in the decrease of its catalytic activity for tar cracking [47,55]. Dolomite can be deactivated by hydration and carbonation reactions [75].

Syngas cleaning processes are classified in two types depending on their location; either in the gasifier (primary methods) or downstream of the gasifier (secondary methods) [77]. Secondary methods may be slightly more efficient than primary ones but a specific catalytic cracking reactor is required thus increasing the investment and operating costs of the gasification unit. Dolomite as in-bed material was shown to be an efficient catalyst for tar cracking [49] allowing the production of a relatively clean syngas. For this reason, dolomite is often used as bed material in gasification and notably in many recent studies [78–81].

In fluidized bed gasifier, dolomite is in contact with biomass particles, and a modification of its surface properties is likely to occur. These modifications could change the long-term

catalytic activity of "used dolomite" for tar cracking, thus modifying the syngas yield and quality. This crucial topic has never yet been explored for dolomite whereas it has been extensively studied for olivine. Indeed, several studies showed that olivine is coated by ash materials during biomass gasification and this ash layer considerably increases the reactivity of olivine for tar cracking and WGS reactions [82–88]. This present work reveals that the impact of ashes may be very different for dolomite than for olivine.

To the best of our knowledge, this work presents for the first time the effect of dolomite aging under significant gasification conditions (in a pilot plant) on tar conversion. Dolomites before and after gasification of biomass were characterized by complementary methods (BET, SEM-EDX, XRD, XPS, TPO, TPD). Then the reactivity of these 2 dolomites (pristine and used) was studied by a "probe" key reaction of tar conversion which is the steam reforming of benzene. Finally the mechanisms of benzene steam reforming over dolomites are discussed.

2. Materials & Methods

2.1. Presentation of the dolomite samples

The dolomite originating from Cantabria (Spain) was calcined at 1000°C for few hours before being used as a catalyst in a biomass gasification plant at Portalegre, Portugal (EQTEC technology) [89]. The gasification reactor was a dense fluidized bed operated at a temperature of 750°C for 10 days using air as gasifying agent. Biomass was a mixture of wood (70%) and miscanthus (30%) and was fed in the reactor at a flow-rate of 50kg/h. The analysis of biomass is presented in supplementary material. The dolomite samples were denoted as "fresh" after calcination, and "used" after gasification. Both samples were sieved to particle sizes from 100 to 250μm.

2.2. Characterizations of the catalysts

The morphology of fresh and used dolomite materials was studied on a scanning electron microscope (SEM) JEOL model JSM-6490LV combined with energy dispersive X-ray spectroscopy (EDX) to analyse the chemical composition of the surface.

For inductively coupled plasma mass spectrometry (ICP-MS) analysis of the bulk, the samples were dissolved in lithium metaborate ($LiBO_2$) and nitric acid (HNO_3) solutions following the CNRS-SARM procedure [90].

The crystalline structure of the fresh and used dolomites was analysed by X-ray diffraction (XRD) measurements. XRD analyses were performed at room temperature using a Philips Panalytical X'Pert Pro MPD diffractometer equipped with Xcelerator detector. XRD

147 patterns were collected with a CuKα radiation source operating at 40kV and 40mA. The
148 diffraction pattern was collected in the range 2θ = 10-80°, with a step size of 0.016° in 2θ, and a
149 scan speed of 1.7min^{-1}.

150 XPS analyses were performed using a KRATOS Axis Ultra X-ray photoelectron
151 spectrometer (Kratos Analytical, Manchester, UK) equipped with a monochromatic Al Kα X-ray
152 source (hν=1486.6eV) operated at 150W. Spectra were collected at normal (90°) take-off angle
153 and the analysis area was 700×300μm. The base pressure in the analytical chamber was 10^{-9}mbar
154 during XPS measurements. Wide scans were recorded using an analyser pass energy of 160eV,
155 while narrow scans were obtained using a pass energy of 20eV (instrumental resolution better
156 than 0.5eV).

157 BET areas were determined by the one-point method using adsorbed nitrogen at 77K in a
158 Micromeritics TriStart II instrument. The solids were previously degassed under vacuum at room
159 temperature overnight.

160 Temperature Programmed Desorption (TPD) and Temperature Programmed Oxidation
161 (TPO) were performed by heating the dolomite samples at 850°C under a 30 NmL/min flow of
162 pure nitrogen (TPD) or air (TPO). A 2.5g dolomite sample was placed in a quartz U-reactor
163 (internal diameter=10mm) heated by an electrical furnace at 5°C/min to 850°C. The exhaust gas
164 was analysed online by a micro-gas chromatograph (μGC) (SRA Instrumentation R3000).

165 **2.3. Catalytic experiments**

166 The experiment set-up has been presented previously [91]. Catalytic experiments were
167 conducted on a fixed bed quartz reactor (internal diameter 10mm) placed in an electric oven. The
168 catalytic bed was supported by a quartz sintered plate. A thermocouple was positioned within the
169 bed of dolomite. The inlet gas composition was controlled by mass flow controllers
170 (Bronkhorst). Benzene (supplied by Fluka, 99.9% purity) and demineralised water were added in
171 the gas mixture by two syringe pumps and vaporised in a vaporisation chamber, swept by
172 nitrogen and connected through a heated line to the catalytic bed. At the outlet of the catalytic
173 bed, permanent gases were analysed on-line with a μ-GC Varian 490 equipped with 4 modules.
174 The outlet was also connected to a heated sampling line and to a heated sampling loop for on-
175 line analysis of benzene by a GC/FID.

176 The operating conditions of the catalytic tests were chosen in order to obtain a contact
177 time similar to the one used in the industrial gasification fluidized bed of EQTEC. The mass of
178 catalyst was 3.0g and the total gas flow rate was set at 45NmL/min. These conditions were set to
179 be consistent with the industrial fluidized bed conditions (mass of fluidized dolomite bed and
180 total outlet syngas flow rate). The benzene inlet concentration was 0.5vol% which corresponds to

the content usually measured in the syngas [3]. Catalytic tests were performed at 800, 850 and 900°C without applying pre-treatment to the materials. The conversion of benzene was constant over time on stream and the value presented is an average of several points (GC/FID analysis) over more than 50 minutes.

The benzene conversion (X_B) was calculated according to Eq.1, where $\dot{n}_B^{in}$ is the molar flow rate of benzene feeding the reactor, and $\dot{n}_B^{out}$ the molar flow rate of benzene leaving the reactor.

$$X_B = \frac{\dot{n}_B^{in} - \dot{n}_B^{out}}{\dot{n}_B^{in}} . 100 \qquad \text{Eq.1}$$

The selectivity (S_i) of the reaction products (i) was also calculated according to Eq.2:

$$S_i = \frac{\dot{n}_i^{out}}{\dot{n}_B^{in} - \dot{n}_B^{out}} . 100 \qquad \text{Eq.2}$$

3. Results and discussion

3.1. Characterization of the catalysts

3.1.1. Morphology of particles and chemical composition of the bulk catalysts by ICP

Table 1 compares the values of BET surface area of fresh and used dolomite samples. For fresh dolomite, the measured values were not high enough to be accurate. Both types of catalysts exhibited low BET surface areas (< 20m²/g). However, a slight increase of the BET surface area was observed for used dolomite samples.

Table 1. BET surface area of dolomite and olivine.

Catalyst	BET (m^2/g)
Fresh dolomite	0.4
Used dolomite	19.5

SEM images and EDX analyses of dolomite materials are presented in Figure 1 and Table 2. EDX analysis was averaged on various particles. Dolomite is a natural material and presents an average composition of about 17% Mg and 34% Ca. After its use as a bed material in the fluidised bed reactor, the surface of used dolomite is enriched by inorganic elements initially contained in the biomass. The surface of dolomite particles is coated by a layer of ashes and becomes smoother as shown on Figure 1. The mechanisms of coating are out of the scope of the present study and have been previously studied in details [3,92,93]. The coating behaviour

depends on gasification conditions and on the composition of the bed, the reactor walls and the ashes of biomass.

Si and P are not detected on fresh dolomite, but their concentrations at the surface of used dolomite are of about 2.5 and 3.7wt.% respectively (Table 2). SEM-EDX is only a first qualitative approach of dolomites chemistry. For this reason, ICP-MS, XRD, XPS and TPD/TPO analyses were performed in order to study more deeply the chemical composition of the catalysts.

Table 2. SEM-EDX analysis of fresh and used dolomite

	Fresh dolomite			Used dolomite		
Elements (wt.%)	Min	**Average**	Max	Min	**Average**	Max
O	44.7	**49.4**	59.8	41.1	**48.1**	54.8
Mg	1.6	**17.0**	36.2	3.6	**5.3**	7.5
Ca	19.1	**33.7**	48.5	37.0	**41.9**	46.6
P	*nd*	***nd***	*nd*	2.2	**2.5**	2.7
Si	*nd*	***nd***	*nd*	3.3	**3.7**	4.1

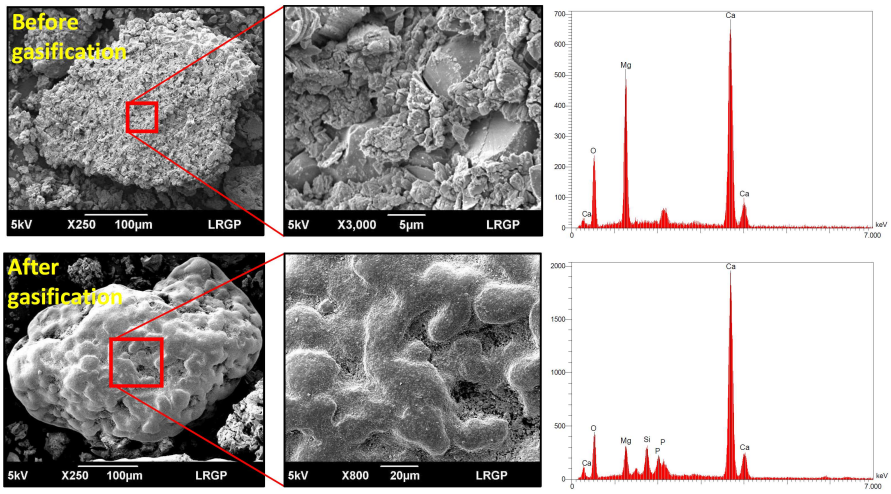

Figure 1. SEM-EDX analysis of the 2 dolomites (before and after biomass gasification in a pilot scale gasifier). SEM-EDX highlights the modification of the surface of particles which are coated by a layer of ashes during biomass gasification.

Table 3 presents the bulk chemical composition of the catalysts analyzed by ICP-MS. These results confirm that used catalysts were enriched in inorganic species during the biomass gasification. Fresh dolomite is mainly composed of CaO (50%) and MgO (38%), with some traces of iron, silicium and aluminium (presented as oxides due to the ICP analysis). After gasification, used dolomite is mainly enriched in SiO_2 (4.3 wt.%, which is similar to EDX analysis)

227 and P_2O_5 (0.39 wt.%, which is lower than EDX analysis). The two main species, CaO and MgO,
228 were found to decrease mainly due to the increase of SiO_2, while Al_2O_3 (1.02 wt.%) slightly
229 increased in used dolomite. The loss on ignition increased for used dolomite (from 9.01 to
230 11.88wt.%) as a result of coke deposit and carbonates. Other species present in biomass ashes
231 (K, Mn, etc.) are also present in higher amount in the used dolomite which is in agreement with
232 ash composition of biomass (presented in supplementary material). Ash composition depends on
233 biomass type and culture mode but these elements are often found as the main inorganic
234 elements of many ligno-cellulosic biomasses. Therefore this ash coating is representative and
235 significant for the gasification of various biomasses in air-dense fluidized bed.
236
237 Table 3. Elemental composition of fresh and used dolomite (obtained by ICP-MS).

Element (wt.%)	**Fresh dolomite**	**Used dolomite**
Loss on ignition (wt.%)	9.01	11.88
SiO_2	0.53	4.35
Al_2O_3	0.26	1.02
Fe_2O_3	0.39	0.43
MnO	0.02	0.14
MgO	38.30	34.16
CaO	50.13	47.20
Na_2O	0.02	0.04
K_2O	0.01	0.28
TiO_2	0.02	0.05
P_2O_5	0.03	0.39

238

239 *3.1.2. XRD characterization of the catalysts*
240
241 As observed in Figure 2, the diffraction peaks of fresh dolomite show the presence of
242 periclase (MgO), lime (CaO), and portlandite ($Ca(OH)_2$). The peaks representative of dolomite
243 structure ($CaMg(CO_3)_2$) are not detected. This crystalline modification can be explained by the
244 effect of the calcination treatment initially applied to this material, which is in agreement with
245 previous studies [45,65]. The XRD spectrum of used dolomite reveals the formation of
246 significant amounts of quartz (SiO_2) and traces of corundum (Al_2O_3). This evolution corroborates
247 the ICP and SEM-EDX results demonstrating the enrichment of ash-based species in dolomite
248 particles during biomass gasification. XRD analysis also shows a relative decrease of MgO vs.
249 CaO in used dolomite. A small peak of calcite is detected in the used dolomite probably due to a
250 limited carbonation at 750°C in the gasifier (around 15%vol. of CO_2 at the exit of the fluidised
251 bed).

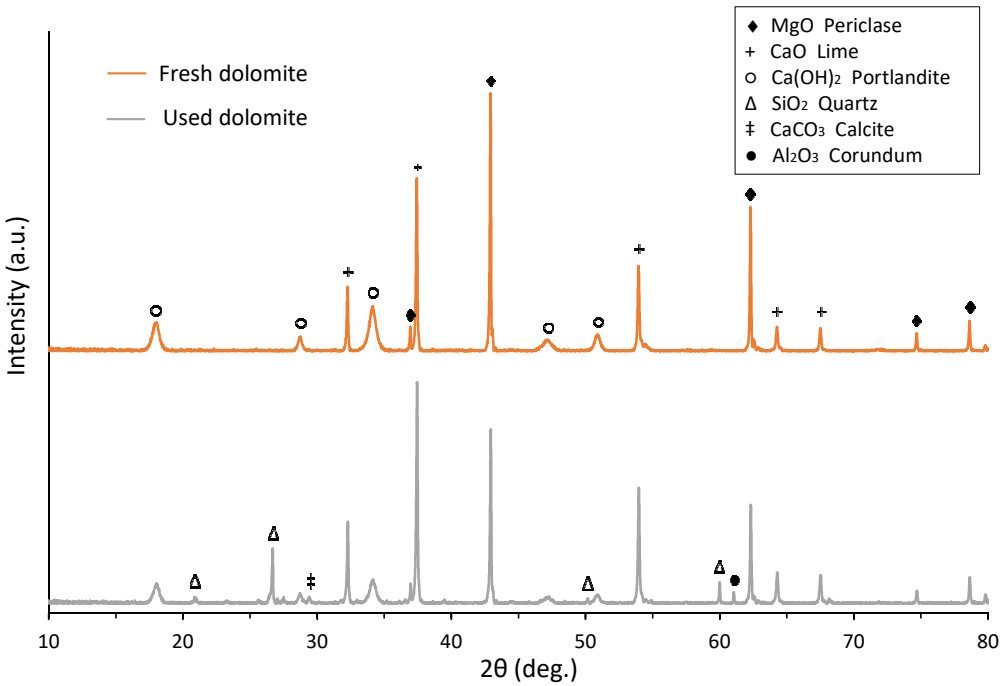

Figure 2. Diffractogram of the fresh and used dolomites

3.1.3. Composition of the surface by XPS

The XPS results are presented in Table 4. Binding energy (BE) and atomic concentration (%) were ascribed to the element according to published data [45,94,95].

For fresh dolomite, the binding energies of the C *1s* signal (Table 4) highlight the presence of various carbonaceous species: graphitic or/and aliphatic hydrocarbons (C-C, C-H) at 284.6 eV, ethers (C-O) at 286.02 eV, aldehydes or carboxylic acids (C=O) at 287.89 eV, and carbonates ($(CO_3)^{2-}$) at 289.40 eV. Carbonates are part of the dolomite composition and are present in higher relative amount on the surface than in the bulk (as shown by XRD) mainly explained by the exposure to air (at room temperature) of the decarbonated samples. The other carbon species than carbonates may be attributed to carbonaceous deposit [94].

Two oxygen species were observed through the O *1s* binding energies at 531.17eV and 532.80 eV. The first one corresponds to O-C or O-H bonds, related to the presence of both carbonaceous and hydroxyl species [95]. These 2 types of bonds unfortunately cannot be discriminated. The second O *1s* signal at 532.80eV is generally attributed to chemisorbed water [95]. However, the high percentage of 40.47% is much higher than that of the carbonaceous species identified by the C-O bonding at 286.02 eV. Therefore the O *1s* binding at 531.17eV may rather correspond to structural hydroxyls of the fresh catalyst. Its surface would be highly hydroxylated probably due to room temperature storage.

The Mg *2p* and Ca *2p* signals correspond to surface concentrations (13.56 and 1.86% respectively) much lower than the bulk oxides as analyzed by ICP. This result may be related to the highly hydroxylated surface of the catalyst.

While iron and aluminium were observed in the bulk by ICP (0.4 and 1.0%, respectively), these elements are not detected at the surface of dolomite by XPS (before and after gasification). Their content may be beyond the detection limit of the XPS technique, or these species could be mainly located in the bulk and not at the external surface analysed by XPS.

Concerning the used dolomite, silica species are found at the surface (1.0%) which is consistent with SEM-EDX analysis. The Mg *2p* and Ca *2p* intensity peaks decrease after gasification: their atomic ratio dropped from 13.56 to 9.72 at.% for Ca, and from 1.86 to 1.00 at.% for Mg (Table 4). This relative decrease in Ca and Mg is consistent with the bulk analysis by ICP measurements (Table 3).

Table 4. XPS analysis of fresh and used dolomites

Element	**Fresh Dolomite**		**Used Dolomite**	
	BE (eV)	**at.%**	**BE (eV)**	**at.%**
O 1s O-C/O-H	531.17	40.47	532.16	27.59
O 1s H_2O	532.80	5.33	533.66	6.68
C 1s C-(C,H)	284.60	23.88	284.59	23.00
C 1s C-OR, C-OH, C-O	286.02	3.32	285.72	16.49
C 1s C=O	287.89	1.25	287.14	5.75
C 1s CO_3^{-2}	289.40	10.33	290.24	8.74
Ca 2p	346.80	13.56	347.75	9.72
Mg 2p	49.40	1.86	50.35	1.03
Si 2p	-	-	101.25	1.00

The evolution of the oxygenated and carbonaceous species observed with XPS after gasification is illustrated in Figure 3. After gasification the atomic concentration of carbon at the surface of used dolomite significantly increases (from 38.8 to 53.9 wt.%), and the concentration of oxygen drops from 45.8 to 34.3 wt.%. Carbonaceous species containing ethers or carboxylic functions strongly increase after gasification (from 3.32 to 16.49%, and from 1.25 to 5.75%, respectively) probably due to oxygenated carbon deposit (Table 4). The content of hydrocarbons originally contained in the dolomite structure (C 1s C-(C-H)) is almost unchanged. The concentration of carbonates (C 1s CO_3^{2-})) decreases a little after gasification. O 1s signal considerably decreases after gasification. Globally, after gasification, the surface becomes richer in C-O species and poorer in Ca-O and Mg-O.

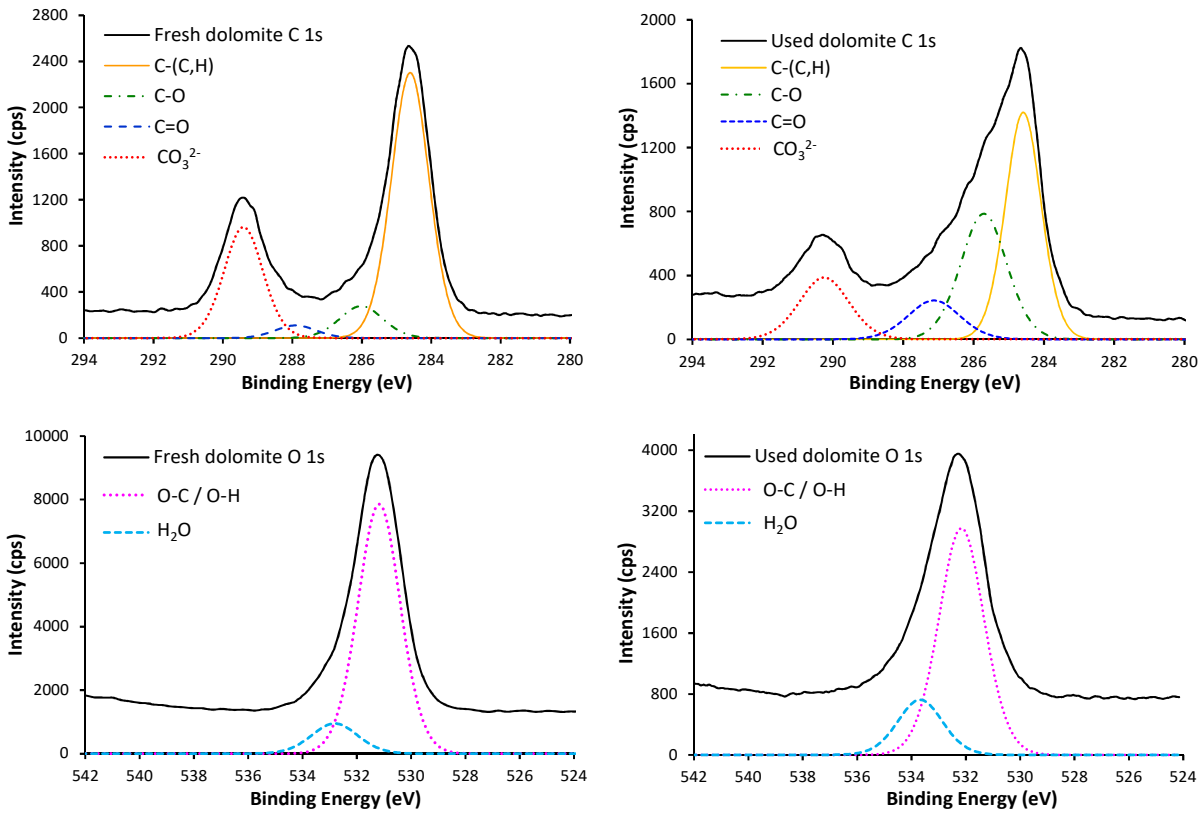

Figure 3. XPS spectra of carbon (C 1s) and oxygen (O 1s) species analysed on fresh dolomite and used dolomite after gasification.

TPD and TPO experiments were performed in order to complete these XPS analysis and to get a better insight on the nature of carbonaceous species present in fresh and used dolomites.

3.1.4. TPD and TPO characterizations

The amounts of CO_2 released by fresh and used dolomite during TPD and TPO analysis are presented in Figure 4 (A) and (B) respectively.

No carbon monoxide was released during these analyses. During TPD (Figure 4A), both samples display a single CO_2 peak occurring at a similar temperature (between 500 and 750°C). The maximum peak is at 660°C and 715°C for fresh dolomite and used dolomite, respectively. The CO_2 release obtained under pure nitrogen atmosphere is attributed to the decomposition of carbonates present in both samples. It can be noted that the amount of CO_2 desorbed was significantly higher for the used dolomite, which could be explained by the formation of carbonates during the gasification reactions. This is in agreement with XRD analysis (Figure 2).

During the TPO analysis, a significant CO_2 peak is obtained at low temperature (460°C) for used dolomite (Figure 4B). This peak results from the oxidation of a reactive carbon

produced during gasification. In addition, a CO_2 peak similar to that obtained during the TPD tests is observed for both samples. However, for used dolomite, the maximum of this peak is achieved at slightly higher temperature than during TPD (790°C vs 715°C), and the amount of CO_2 released is much higher. This difference can be attributed to the oxidation of a more stable coke produced during the gasification reactions and oxidized at high temperature (≈800°C). To the best of our knowledge we present here the first TPO analysis of a dolomite used in a pilot scale gasifier during a significant time (10 days).

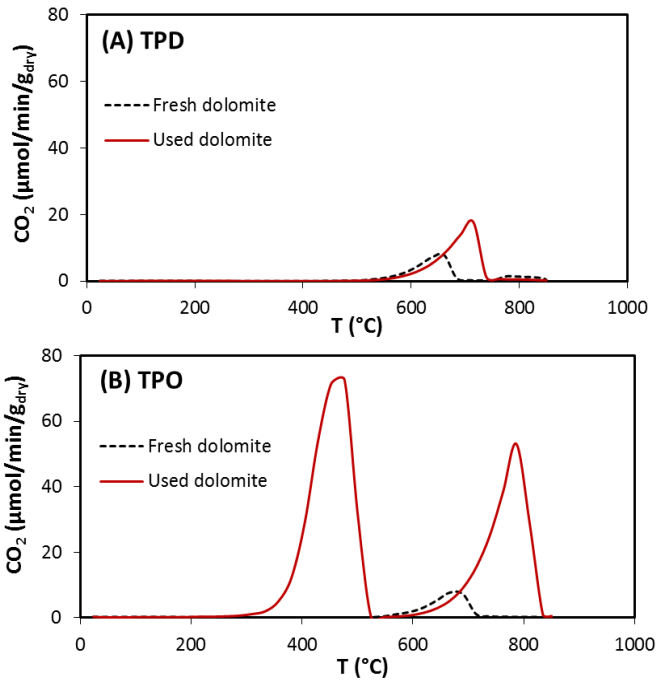

Figure 4. (A) TPD and (B) TPO analysis of fresh and used dolomites.

It is interesting to notice that similar ratios of carbonates to total carbon [$C_{Carbonates}/C_{total}$] were found between TPD/TPO ($C_{Carbonates}/C_{total}$=0.13) and XPS ($C_{Carbonates}/C_{total}$=0.16) for the used dolomite. This would mean that the evolution of CO_2 analysed during TPD/TPO may account for the decomposition of functions (carbonates and coke deposit) which are mainly formed at the external surface of particles during biomass gasification.

3.2. Steam reforming of benzene over fresh and used dolomites

In order to "probe" the reactivity of the two dolomite samples, their catalytic activity for benzene steam reforming were compared at three temperatures (800, 850 and 900°C). The evolution of benzene conversion is presented in Figure 5.

For both dolomites, the increase in temperature increases the benzene conversion. Indeed, the conversion of benzene is multiplied by 3.5 between 800 and 900°C. It is interesting to note that used dolomite is less active than the fresh one. The activity of used dolomite decreases by about 25% compared to the fresh sample. At 900°C the conversion of benzene obtained with fresh dolomite reaches 70% against 54% with used dolomite.

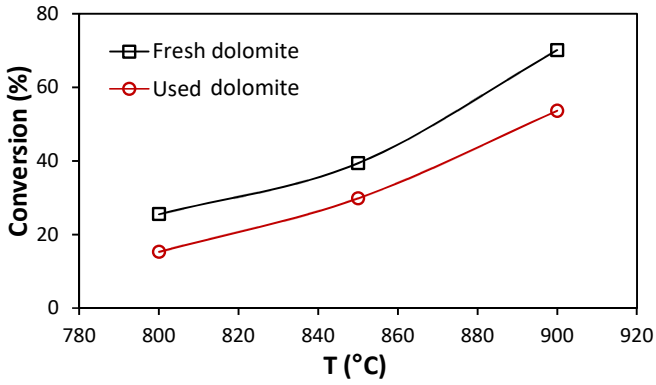

Figure 5. Effect of temperature and dolomite aging on benzene conversion during steam reforming (C_6H_6=0.5 vol%, H_2O=22.2 vol% in N_2, 3 g dolomite, 45 NmL/min total flow rate).

To assess the effect of aging on the reaction mechanisms, the selectivity on reaction products has been determined (Table 5). Similar gaseous species were produced by fresh and used dolomites: H_2, CO_2, CO, and CH_4. For both samples, the main products were H_2 and CO_2. Traces of C_2H_4 were produced by steam reforming of benzene only over the fresh dolomite.

For fresh dolomite, rising temperature from 800 to 900°C results in a decrease of H_2 (-3.9%) and CO_2 (-2.3%) selectivities at the expense of CO (+3.7%) and CH_4 (+2.5%). This means that the overall selectivity in products is not mainly controlled by the thermodynamic equilibrium of the water gas-shift reaction which promotes H_2 and CO_2 at lower temperatures. The increase in CO/CO_2 with temperature is in agreement with results reported by *Constantinou et al.* in a stream rich in H_2 [45]. At higher temperature, the cracking reaction of benzene forming CH_4 seems to be promoted. The decrease in H_2 selectivity with temperature may be linked to the higher selectivity in CH_4. Further discussion is provided after the presentation of a potential mechanism of benzene reforming over dolomites in the next section.

Table 5. Molar selectivity of the products generated by steam reforming of benzene.

	H_2 (mol%)			CO_2 (mol%)			CO (mol%)			CH_4 (mol%)			C_2H_4 (mol%)		
T (°C)	800	850	900	800	850	900	800	850	900	800	850	900	800	850	900
Fresh dolomite	66.9	65.8	63.0	25.7	25.2	23.4	1.9	3.1	5.6	3.0	4.4	5.5	0.8	0.9	0.6
Used dolomite	65.5	66.9	66.5	30.7	27.4	22.4	2.6	3.5	8.3	1.2	2.2	2.9	0.0	0.0	0.0

Concerning the used dolomite, the evolutions of CO_2 and CO are more significant with rising temperature: -8.3% and +5.6%, respectively. Contrary to the fresh dolomite, the selectivity in H_2 was almost constant with rising temperature. This finding confirms that the equilibrium of water gas-shift reaction does not control the global selectivity in $CO_2/H_2/CO$ in this case. The steam gasification of coke present in the used dolomite (deposited during biomass gasification and as analyzed by TPO) may also contribute the higher selectivity in H_2 and CO notably at 900°C. More complex phenomena occur and will be detailed in the next section. The selectivities in CH_4 and in C_2H_4 are lower for the used dolomites. This result may be explained by a lower cracking rate of benzene over the used dolomite.

3.3. Discussion on the reaction mechanisms

In a deep study *Alarcon et al.* have proposed a detailed mechanism for the steam reforming of aromatics over CaO and MgO [68]. These authors have proposed, by analogy with the mechanism of hydrocarbons steam-reforming over metal supported catalysts [96], that aromatic hydrocarbons reforming over CaO or MgO catalysts would take place in two main step [94]: (i) the decomposition of the hydrocarbon and the water on the catalyst surface, and then (ii) the gasification of the deposited carbon with steam. The overall process could be written according to the following simplified mechanism:

$$ArH + \star \rightarrow C_xH_y\text{-}\star \quad \text{(R1)}$$

$$H_2O + \star \rightarrow O\text{-}\star + H_2 \quad \text{(R2)}$$

$$C_xH_y\text{-}\star + O\text{-}\star \rightarrow H_2, CO, CO_2, CH_4 + 2\star \quad \text{(R3)}$$

where ArH is an aromatic hydrocarbon specie, $\star$ is a $M^{2+}O^{2-}$ unit (the active site in dolomite). The deposit (C_xH_y-) may also decompose into smaller fragments and further form H_2, CH_4, and C_x [68,94].

The decomposition of water molecules to hydrogen is easy over metal supported catalyst when the metal phase is a noble or transition metal [96]. This is much less likely to occur over the

389 non-reducible CaO or MgO oxides, unless they contained catalytic traces of a transition metal (e;
390 g; iron). Contrary to the reaction (R2) proposed by a previous study, we rather think that gaseous
391 H_2 stems from the decomposition of gaseous water on the carbon fragments rather than from
392 the direct water decomposition on the metal oxides. In other words, the water molecules are
393 reduced by the surface carbon fragments but not by the fixed valence metal oxides.

394 Based on our results and on literature analysis [45,68,74,94,97], an overall mechanism of
395 benzene steam reforming over dolomite is proposed (Figure 6).

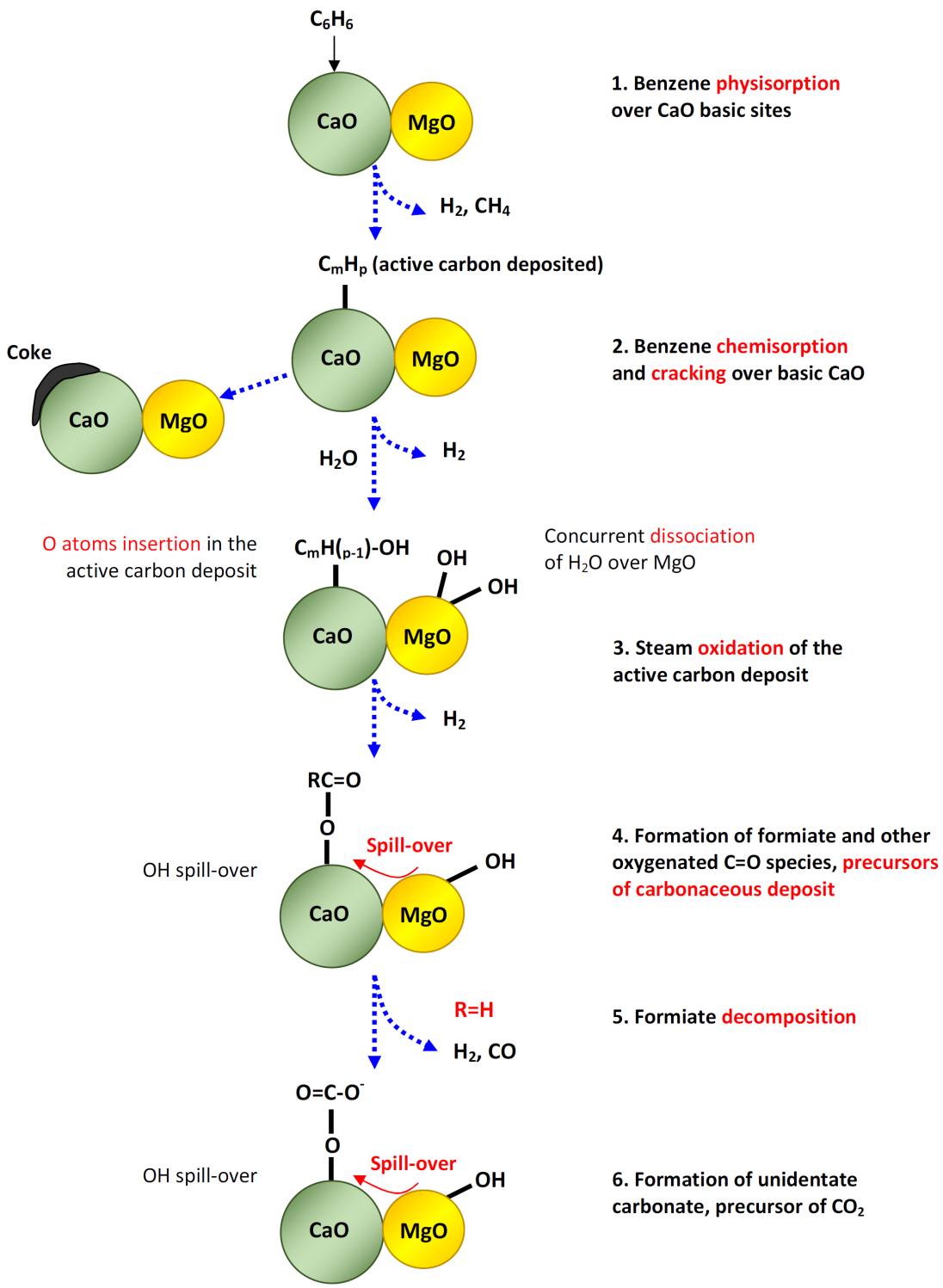

Figure 6. Chemical mechanism of benzene steam reforming over dolomite proposed based on the experimental results of the present study and on previous works [45,68,74,94,97].

First, a theoretical investigation of benzene adsorption over calcite and dolomite dry surfaces reported that Ca sites are the most energetically favorable for hydrocarbon adsorption

402 on both minerals [98]. Moreover, van der Waals interactions increase the stability for all sites but
403 more strongly on the Ca site. The benzene molecule was found to be adsorbed in a Ca hole, the
404 aromatic ring forming an angle of 15 to 35° with the surface. For MgO, benzene adsorption takes
405 place on weakly acidic OH groups, rather than on the Mg sites. The rate determining step of the
406 steam-reforming of benzene over dolomite is the adsorption of the reactant hydrocarbon
407 molecule [69]. This can be explained by the interactions between a neutral molecule and a
408 strongly polarized solid surface. The stable and symmetrical benzene molecule is not easily
409 polarizable, even with the highly ionic CaO or MgO dipoles. As a result, the chemical adsorption
410 is weak and the Van der Waals interactions may become important [99]. From hard and soft acids
411 and bases principles [100,101], benzene is a soft base and Ca^{2+} a hard acid, also their interaction is
412 fundamentally expected to be very poor. This interaction should be of van der Waals type, in
413 good accordance with the theoretical investigation reported by *Rigo et al.* [98]. From these studies,
414 it can be proposed that benzene is rather adsorbed and decomposed on the calcium oxide by
415 interaction with the Ca^{++} component (Figure 6).
416 Second, concerning the adsorption and role of water, MgO, CaO and other non-reducible
417 oxides (activated at high temperatures) exhibit the presence of highly basic O^{2-} sites [97]. The OH
418 groups were shown to exist in the naphthalene steam-reforming reaction conditions over pure
419 MgO or MgO+CaO mixture, but not over pure CaO [68]. On the other hand, the introduction
420 of steam results in the disappearance of the carbonaceous matter (mainly in the form of formiate
421 species) from the surface of pure MgO and MgO-containing mixture, while formiate species
422 remains in the surface of CaO catalyst [68]. The authors concluded that the OH groups,
423 stemming from MgO, could participate both to the gaseous products formation and to coke
424 removal. Chemically, it is impossible that anionic OH groups directly participate to the oxidation
425 of carbons belonging to C-C or C-H σ bonds. Thus, OH^- cannot be active species in the benzene
426 steam-reforming. On the contrary, H_2O may be responsible for the direct oxidation of
427 hydrocarbons ($C_mH_{(p-1)}$-OH) (Figure 6). Due to its chemical properties, OH^- can be reactive
428 towards the oxidation of the carbon of C=O double π bonds of oxygenate species by a
429 nucleophilic attack. The presence of these species over alkaline oxides were evidenced by *Alarcon*
430 *et al.* [94]. These species disappear from the surface after the introduction of steam in the reactor
431 over MgO or CaO+MgO, but not over pure CaO. This led us to conclude that the role of MgO
432 in MgO+CaO mixture (and therefore in dolomite) is to bring the OH groups for the oxidation of
433 oxygenate species deposited over CaO (after benzene sorption). This reaction would occur at the
434 MgO-CaO interface or through the spillover effect of the OH groups [102] (Figure 6).

In an investigation on MgO [99] prepared from $Mg(OH)_2$ precursor treated at various temperatures, it was shown that the surface OH concentration was similar for small or large MgO particles, but that the latter allowed more germinal OH pairs as well as OH surface island domains with weak Brönsted acidity. The reactivity of the OH groups is thus related to the morphology of MgO which, in turn, depends on the nature of the precursor and pre-treatments. This may contribute to the difference of reactivity of MgO in MgO+CaO mechanical mixture, and dolomite.

Therefore in our proposed mechanism (Figure 6), the first step consists in the adsorption of benzene over the basic site of CaO [98] to form an active carbon deposit (C_mH_p), C_xH_Y gas species (as analyzed in our work), and H_2. Then, the active carbon deposit can produce coke. Water may either directly oxidize this active carbon deposit or may be dissociatively chemisorbed over MgO active site to form OH basic species. These OH basic species contribute to the formation of formiate and other oxygenate intermediates, then forming unidentate carbonate through OH spill-over. Formiate and carbonates have been analyzed by XPS in this present work and by infrared spectroscopy by *Alarcon et al.* [68,94] and *Constantinou et al.* [45]. This mechanism corroborates the results of *Constantinou et al.* [45] who demonstrated that OH species are important reaction intermediates for the conversion of aromatics into C_x and H_2. It has also been proved that unidentate carbonates are less stable than bicarbonates and constitute the main species formed over dolomite [45,68,103]. The former would be the precursors in CO_2 formation.

The proposed mechanism supports our experimental results. When the temperature increases, the cracking of benzene promotes the formation of C_xH_y gas species, especially over fresh dolomite. This reaction is less favored with the used dolomite probably due to the lower availability of CaO sites (as analyzed by XPS). The temperature increase is also associated to a decrease in CO_2 and an increase in CO selectivities (Table 5). This evolution maybe explained by the cracking of benzene, as well as by the complex coupling between OH species formation and spill-over leading to CO/CO_2 (from formiate and carbonate intermediate). Carbon monoxide is generated by the thermal decomposition of formiate and higher homologs. This reaction was enhanced by increasing temperature, at the expense of the carbonates and CO_2 route. Indeed, at high temperature, this route (formation of OH by H_2O dissociation on MgO sites, and OH spill-over) maybe slower than the formiate thermal decomposition microkinetic rate. Therefore the OH source may be limited leading to a lower formation of CO_2 from carbonate. This effect is even more marked for the used dolomite since MgO sites, required for OH species formation, are expected to be less available. The CO_2 route is also inhibited by increasing cracking reactions

with rising temperature. Further studies are needed to study more deeply the detailed chemistry of these intermediate C-O species at the temperatures of hydrocarbons steam reforming.

For used dolomite, the deposit of coke and ashes, detected in this study by various analytical tools, reduced the global availability of CaO and MgO active sites, as presented in the simplified scheme in Figure 7.

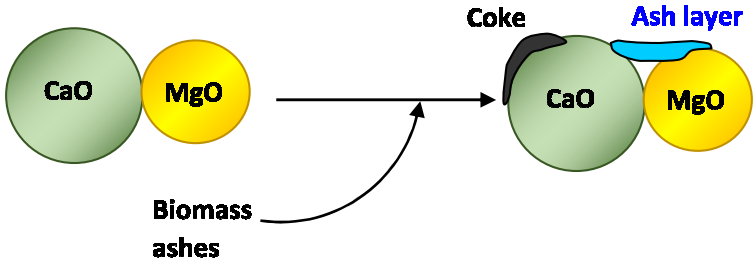

Figure 7. Deactivation of dolomites in biomass gasification reactors: the ashes formed from biomass oxidation leads to a deposit of Si (and other species present in ashes) layer over dolomite, and coke deposit also reduces the available active sites for benzene and water adsorption.

4. Conclusion

The evolution of dolomite surface chemistry during its use as bed material in a pilot-scale gasification reactor and its resulting activity on tar reforming have been studied for the first time. Benzene steam reforming was selected as a model reaction in order to probe the activity of the dolomites.

BET, SEM-EDX, XRD, XPS, and TPO/TPD analyses revealed a drastic change of the surface properties of used dolomites. After being used as a bed material, used dolomite was covered by a layer rich in Si from biomass ash. In addition, coke was deposited at the used dolomite surface after gasification reactions.

The catalytic activity of used dolomite was ≈24% lower than that of fresh dolomite. This drop in catalytic activity can be attributed to the Si-rich layer covering the surface of used dolomite together with the coke deposition which decreased the availability of the active sites (CaO, MgO). In addition, SiO_2 has low catalytic activity towards tar reforming reactions. The SiO_2 and coke deposition could also limit the interactions between CaO and MgO, thus allowing the production of stable coke deactivating the catalyst.

This study presents a methodological approach that can be further used to study the effect of different operating conditions during biomass gasification on the activity and composition of dolomites (or other materials). Based on our experimental results and on the literature data, a new reaction mechanism of benzene steam reforming on fresh and used dolomite was proposed.

Acknowledgements

The ANR agency is thanked for a part of the financial support through the project Gameco (coordinated by EDF). EDF (O. Authier) is acknowledged for having promoted this study and EQTEC for providing the dolomite materials.

References

[1] A.V. Bridgwater, Renewable fuels and chemicals by thermal processing of biomass, Chem. Eng. J. 91 (2003) 87–102.

[2] T.A. Milne, R.. Evans, N. Abatzoglou, Biomass Gasifier Tars: Their Nature, Formation and Conversion., National Renewable Energy Laboratory, 1998.

[3] G. Lardier, J. Kaknics, A. Dufour, R. Michel, B. Cluet, O. Authier, J. Poirier, G. Mauviel, Gas and Bed Axial Composition in a Bubbling Fluidized Bed Gasifier: Results with Miscanthus and Olivine, Energy Fuels. 30 (2016) 8316–8326. doi:10.1021/acs.energyfuels.6b01816.

[4] M. Nowakowska, O. Herbinet, A. Dufour, P.-A. Glaude, Kinetic Study of the Pyrolysis and Oxidation of Guaiacol, J. Phys. Chem. A. (2018). doi:10.1021/acs.jpca.8b06301.

[5] R. Coll, J. Salvadó, X. Farriol, D. Montané, Steam reforming model compounds of biomass gasification tars: conversion at different operating conditions and tendency towards coke formation, Fuel Process. Technol. 74 (2001) 19–31. doi:10.1016/S0378-3820(01)00214-4.

[6] GE Jenbacher, Fuel gas quality, special gases, 2009.

[7] L. Le Coq, A. Duga, Syngas treatment unit for small scale gasification-application to IC engine gas quality requirement, J. Appl. Fluid Mech. 5 (2012) 95–103.

[8] W. Torres, S.S. Pansare, J.G.G. Jr, Hot Gas Removal of Tars, Ammonia, and Hydrogen Sulfide from Biomass Gasification Gas, Catal. Rev. 49 (2007) 407–456. doi:10.1080/01614940701375134.

[9] D. Sutton, B. Kelleher, J.R. Ross, Review of literature on catalysts for biomass gasification, Fuel Process. Technol. 73 (2001) 155–173.

[10] P.J. Woolcock, R.C. Brown, A review of cleaning technologies for biomass-derived syngas, Biomass Bioenergy. 52 (2013) 54–84. doi:10.1016/j.biombioe.2013.02.036.

[11] M.L. Valderrama Rios, A.M. González, E.E.S. Lora, O.A. Almazán del Olmo, Reduction of tar generated during biomass gasification: A review, Biomass Bioenergy. 108 (2018) 345–370. doi:10.1016/j.biombioe.2017.12.002.

[12] Y. Shen, K. Yoshikawa, Recent progresses in catalytic tar elimination during biomass gasification or pyrolysis—A review, Renew. Sustain. Energy Rev. 21 (2013) 371–392. doi:10.1016/j.rser.2012.12.062.

[13] Z. Abu El-Rub, E.A. Bramer, G. Brem, Review of Catalysts for Tar Elimination in Biomass Gasification Processes, Ind. Eng. Chem. Res. 43 (2004) 6911–6919. doi:10.1021/ie0498403.

[14] S. Anis, Z.A. Zainal, Tar reduction in biomass producer gas via mechanical, catalytic and thermal methods: A review, Renew. Sustain. Energy Rev. 15 (2011) 2355–2377. doi:10.1016/j.rser.2011.02.018.

[15] M. Asadullah, Barriers of commercial power generation using biomass gasification gas: A review, Renew. Sustain. Energy Rev. 29 (2014) 201–215. doi:10.1016/j.rser.2013.08.074.

[16] D.A. Bulushev, J.R.H. Ross, Catalysis for conversion of biomass to fuels via pyrolysis and gasification: A review, Catal. Today. 171 (2011) 1–13. doi:10.1016/j.cattod.2011.02.005.

[17] D. Dayton, A review of the literature on catalytic biomass tar destruction, NREL Rep. NRELTP-510-32815 NREL Gold. CO. (2002). http://gekgasifier.pbworks.com/f/CatalyticBiomassLitReview.pdf (accessed January 23, 2014).

[18] L. Devi, K.J. Ptasinski, F.J.J.G. Janssen, A review of the primary measures for tar elimination in biomass gasification processes, Biomass Bioenergy. 24 (2003) 125–140. doi:10.1016/S0961-9534(02)00102-2.

[19] G. Guan, M. Kaewpanha, X. Hao, A. Abudula, Catalytic steam reforming of biomass tar: Prospects and challenges, Renew. Sustain. Energy Rev. 58 (2016) 450–461. doi:10.1016/j.rser.2015.12.316.

[20] J. Han, H. Kim, The reduction and control technology of tar during biomass gasification/pyrolysis: An overview, Renew. Sustain. Energy Rev. 12 (2008) 397–416. doi:10.1016/j.rser.2006.07.015.
[21] L. Devi, K.J. Ptasinski, F.J.J.G. Janssen, Pretreated olivine as tar removal catalyst for biomass gasifiers: investigation using naphthalene as model biomass tar, Fuel Process. Technol. 86 (2005) 707–730. doi:10.1016/j.fuproc.2004.07.001.
[22] A. Jess, Mechanisms and kinetics of thermal reactions of aromatic hydrocarbons from pyrolysis of solid fuels, Fuel. 75 (1996) 1441–1448. doi:10.1016/0016-2361(96)00136-6.
[23] C.M. Kinoshita, Y. Wang, J. Zhou, Tar formation under different biomass gasification conditions, J. Anal. Appl. Pyrolysis. 29 (1994) 169–181.
[24] A. Dufour, E. Masson, P. Girods, Y. Rogaume, A. Zoulalian, Evolution of Aromatic Tar Composition in Relation to Methane and Ethylene from Biomass Pyrolysis-Gasification, Energy Fuels. 25 (2011) 4182–4189. doi:10.1021/ef200846g.
[25] Y. Shen, J. Wang, X. Ge, M. Chen, By-products recycling for syngas cleanup in biomass pyrolysis – An overview, Renew. Sustain. Energy Rev. 59 (2016) 1246–1268. doi:10.1016/j.rser.2016.01.077.
[26] J. Park, Y. Lee, C. Ryu, Reduction of primary tar vapor from biomass by hot char particles in fixed bed gasification, Biomass Bioenergy. 90 (2016) 114–121. doi:10.1016/j.biombioe.2016.04.001.
[27] D. Feng, Y. Zhao, Y. Zhang, Z. Zhang, L. Zhang, S. Sun, In-situ steam reforming of biomass tar over sawdust biochar in mild catalytic temperature, Biomass Bioenergy. 107 (2017) 261–270. doi:10.1016/j.biombioe.2017.10.007.
[28] M. Hervy, A. Villot, C. Gérente, D. Pham Minh, E. Weiss-Hortala, A. Nzihou, L. Le Coq, Catalytic cracking of ethylbenzene as tar surrogate using pyrolysis chars from wastes, Biomass Bioenergy. 117 (2018) 86–95. doi:10.1016/j.biombioe.2018.07.020.
[29] P.R. Buchireddy, R.M. Bricka, J. Rodriguez, W. Holmes, Biomass Gasification: Catalytic Removal of Tars over Zeolites and Nickel Supported Zeolites, Energy Fuels. 24 (2010) 2707–2715. doi:10.1021/ef901529d.
[30] D. Yao, H. Yang, H. Chen, P.T. Williams, Investigation of nickel-impregnated zeolite catalysts for hydrogen/syngas production from the catalytic reforming of waste polyethylene, Appl. Catal. B Environ. 227 (2018) 477–487. doi:10.1016/j.apcatb.2018.01.050.
[31] M. Azhar Uddin, H. Tsuda, S. Wu, E. Sasaoka, Catalytic decomposition of biomass tars with iron oxide catalysts, Fuel. 87 (2008) 451–459. doi:10.1016/j.fuel.2007.06.021.
[32] J. Chen, M. Tamura, Y. Nakagawa, K. Okumura, K. Tomishige, Promoting effect of trace Pd on hydrotalcite-derived Ni/Mg/Al catalyst in oxidative steam reforming of biomass tar, Appl. Catal. B Environ. 179 (2015) 412–421. doi:10.1016/j.apcatb.2015.05.042.
[33] S.J. Juutilainen, P.A. Simell, A.O.I. Krause, Zirconia: Selective oxidation catalyst for removal of tar and ammonia from biomass gasification gas, Appl. Catal. B Environ. 62 (2006) 86–92. doi:10.1016/j.apcatb.2005.05.009.
[34] S. Cheah, K.R. Gaston, Y.O. Parent, M.W. Jarvis, T.B. Vinzant, K.M. Smith, N.E. Thornburg, M.R. Nimlos, K.A. Magrini-Bair, Nickel cerium olivine catalyst for catalytic gasification of biomass, Appl. Catal. B Environ. 134–135 (2013) 34–45. doi:10.1016/j.apcatb.2012.12.022.
[35] D.A. Constantinou, M.C. Álvarez-Galván, J.L.G. Fierro, A.M. Efstathiou, Low-temperature conversion of phenol into CO, CO2 and H2 by steam reforming over La-containing supported Rh catalysts, Appl. Catal. B Environ. 117–118 (2012) 81–95. doi:10.1016/j.apcatb.2012.01.005.
[36] L. Wang, Y. Hisada, M. Koike, D. Li, H. Watanabe, Y. Nakagawa, K. Tomishige, Catalyst property of Co–Fe alloy particles in the steam reforming of biomass tar and toluene, Appl. Catal. B Environ. 121–122 (2012) 95–104. doi:10.1016/j.apcatb.2012.03.025.

[37] D. Li, M. Tamura, Y. Nakagawa, K. Tomishige, Metal catalysts for steam reforming of tar derived from the gasification of lignocellulosic biomass, Bioresour. Technol. 178 (2015) 53–64. doi:10.1016/j.biortech.2014.10.010.
[38] K. Raveendran, A. Ganesh, K.C. Khilar, Influence of mineral matter on biomass pyrolysis characteristics, Fuel. 74 (1995) 1812–1822. doi:10.1016/0016-2361(95)80013-8.
[39] N.B. Klinghoffer, M.J. Castaldi, A. Nzihou, Influence of char composition and inorganics on catalytic activity of char from biomass gasification, Fuel. 157 (2015) 37–47. doi:10.1016/j.fuel.2015.04.036.
[40] Y. Shen, P. Zhao, Q. Shao, D. Ma, F. Takahashi, K. Yoshikawa, In-situ catalytic conversion of tar using rice husk char-supported nickel-iron catalysts for biomass pyrolysis/gasification, Appl. Catal. B Environ. 152–153 (2014) 140–151. doi:10.1016/j.apcatb.2014.01.032.
[41] P.H. Blanco, C. Wu, J.A. Onwudili, P.T. Williams, Characterization and evaluation of Ni/SiO2 catalysts for hydrogen production and tar reduction from catalytic steam pyrolysis-reforming of refuse derived fuel, Appl. Catal. B Environ. 134–135 (2013) 238–250. doi:10.1016/j.apcatb.2013.01.016.
[42] J.N. Kuhn, Z. Zhao, L.G. Felix, R.B. Slimane, C.W. Choi, U.S. Ozkan, Olivine catalysts for methane- and tar-steam reforming, Appl. Catal. B Environ. 81 (2008) 14–26. doi:10.1016/j.apcatb.2007.11.040.
[43] M. Virginie, C. Courson, D. Niznansky, N. Chaoui, A. Kiennemann, Characterization and reactivity in toluene reforming of a Fe/olivine catalyst designed for gas cleanup in biomass gasification, Appl. Catal. B Environ. 101 (2010) 90–100. doi:10.1016/j.apcatb.2010.09.011.
[44] J.F. González, S. Román, G. Engo, J.M. Encinar, G. Martínez, Reduction of tars by dolomite cracking during two-stage gasification of olive cake, Biomass Bioenergy. 35 (2011) 4324–4330. doi:10.1016/j.biombioe.2011.08.001.
[45] D.A. Constantinou, J.L.G. Fierro, A.M. Efstathiou, A comparative study of the steam reforming of phenol towards H_2 production over natural calcite, dolomite and olivine materials, Appl. Catal. B Environ. 95 (2010) 255–269. doi:10.1016/j.apcatb.2010.01.003.
[46] M.F. Tennant, D.W. Mazyck, Steam-pyrolysis activation of wood char for superior odorant removal, Carbon. 41 (2003) 2195–2202. doi:10.1016/S0008-6223(03)00211-2.
[47] A. Donnot, P. Magne, X. Deglise, Reactions of Dolomite with CO<Subscript>2</Subscript> at Gasification Temperatures of Wood, in: Res. Thermochem. Biomass Convers., Springer, Dordrecht, 1988: pp. 1002–1015. doi:10.1007/978-94-009-2737-7_75.
[48] P. Pérez, P.M. Aznar, M.A. Caballero, J. Gil, J.A. Martín, J. Corella, Hot Gas Cleaning and Upgrading with a Calcined Dolomite Located Downstream a Biomass Fluidized Bed Gasifier Operating with Steam−Oxygen Mixtures, Energy Fuels. 11 (1997) 1194–1203. doi:10.1021/ef970046m.
[49] J. Corella, M.-P. Aznar, J. Gil, M.A. Caballero, Biomass Gasification in Fluidized Bed: Where To Locate the Dolomite To Improve Gasification?, Energy Fuels. 13 (1999) 1122–1127. doi:10.1021/ef990019r.
[50] J. Delgado, M.P. Aznar, J. Corella, Calcined dolomite, magnesite, and calcite for cleaning hot gas from a fluidized bed biomass gasifier with steam: life and usefulness, Ind. Eng. Chem. Res. 35 (1996) 3637–3643.
[51] G. Taralas, Effects of MgO, CaO and calcined dolomites on model substance cracking and conversion of tar from biomass gasification/pyrolysis gas, Department of Chemical Technology - Royal Institute of Technology, Stockholm, 1990.
[52] P.A. Simell, E.K. Hirvensalo, V.T. Smolander, A.O.I. Krause, Steam Reforming of Gasification Gas Tar over Dolomite with Benzene as a Model Compound, Ind. Eng. Chem. Res. 38 (1999) 1250–1257. doi:10.1021/ie980646o.

[53] H. Aldén, E. Björkman, M. Carlsson, L. Waldheim, Catalytic Cracking of Naphthalene on Dolomite, in: Adv. Thermochem. Biomass Convers., Springer, Dordrecht, 1993: pp. 216–232. doi:10.1007/978-94-011-1336-6_17.

[54] P.A. Simell, N.A.K. Hakala, H.E. Haario, A.O.I. Krause, Catalytic decomposition of gasification gas tar with benzene as the model compound, Ind. Eng. Chem. Res. 36 (1997) 42–51.

[55] P.A. Simell, J.K. Leppälahti, E.A. Kurkela, Tar-decomposing activity of carbonate rocks under high CO2 partial pressure, Fuel. 74 (1995) 938–945. doi:10.1016/0016-2361(95)00012-T.

[56] E. Gusta, A.K. Dalai, M.A. Uddin, E. Sasaoka, Catalytic Decomposition of Biomass Tars with Dolomites, Energy Fuels. 23 (2009) 2264–2272. doi:10.1021/ef8009958.

[57] A. Sarıoğlan, Tar removal on dolomite and steam reforming catalyst: Benzene, toluene and xylene reforming, Int. J. Hydrog. Energy. 37 (2012) 8133–8142. doi:10.1016/j.ijhydene.2012.02.045.

[58] R. Zhang, R.C. Brown, A. Suby, K. Cummer, Catalytic destruction of tar in biomass derived producer gas, Energy Convers. Manag. 45 (2004) 995–1014. doi:10.1016/j.enconman.2003.08.016.

[59] J.M. de Andrés, A. Narros, M.E. Rodríguez, Behaviour of dolomite, olivine and alumina as primary catalysts in air–steam gasification of sewage sludge, Fuel. 90 (2011) 521–527. doi:10.1016/j.fuel.2010.09.043.

[60] P. Ammendola, B. Piriou, L. Lisi, G. Ruoppolo, R. Chirone, G. Russo, Dual bed reactor for the study of catalytic biomass tars conversion, Exp. Therm. Fluid Sci. 34 (2010) 269–274. doi:10.1016/j.expthermflusci.2009.10.019.

[61] D.C. Elliott, E.G. Baker, The effect of catalysis on wood-gasification tar composition, Biomass. 9 (1986) 195–203. doi:10.1016/0144-4565(86)90089-2.

[62] H. Aldén, B.-G. Espenäs, E. Rensfelt, Conversion of Tar in Pyrolysis Gas from Wood Using a Fixed Dolomite Bed, in: A.V. Bridgwater, J.L. Kuester (Eds.), Res. Thermochem. Biomass Convers., Springer Netherlands, Dordrecht, 1988: pp. 987–1001. doi:10.1007/978-94-009-2737-7_74.

[63] K. Sjöström, G. Taralas, L. Liinanki, Sala Dolomite-Catalysed Conversion of Tar from Biomass Pyrolysis, in: A.V. Bridgwater, J.L. Kuester (Eds.), Res. Thermochem. Biomass Convers., Springer Netherlands, Dordrecht, 1988: pp. 974–986. doi:10.1007/978-94-009-2737-7_73.

[64] P.A. Simell, J.K. Leppälahti, J.B. Bredenberg, Catalytic purification of tarry fuel gas with carbonate rocks and ferrous materials, Fuel. 71 (1992) 211–218. doi:10.1016/0016-2361(92)90011-C.

[65] G. Hu, S. Xu, S. Li, C. Xiao, S. Liu, Steam gasification of apricot stones with olivine and dolomite as downstream catalysts, Fuel Process. Technol. 87 (2006) 375–382. doi:10.1016/j.fuproc.2005.07.008.

[66] A.H. Clemens, L.F. Damiano, T.W. Matheson, The effect of calcium on the rate and products of steam gasification of char from low rank coal, Fuel. 77 (1998) 1017–1020. doi:10.1016/S0016-2361(97)00276-7.

[67] J. Delgado, M.P. Aznar, J. Corella, Biomass Gasification with Steam in Fluidized Bed: Effectiveness of CaO, MgO, and CaO−MgO for Hot Raw Gas Cleaning, Ind. Eng. Chem. Res. 36 (1997) 1535–1543. doi:10.1021/ie960273w.

[68] N. Alarcón, X. Garcı□a, M.A. Centeno, P. Ruiz, A. Gordon, New effects during steam gasification of naphthalene: the synergy between CaO and MgO during the catalytic reaction, Appl. Catal. Gen. 267 (2004) 251–265. doi:10.1016/j.apcata.2004.03.010.

[69] P.A. Simell, J.O. Hepola, A.O.I. Krause, Effects of gasification gas components on tar and ammonia decomposition over hot gas cleanup catalysts, Fuel. 76 (1997) 1117–1127. doi:10.1016/S0016-2361(97)00109-9.

[70] G. Taralas, M.G. Kontominas, X. Kakatsios, Modeling the Thermal Destruction of Toluene (C7H8) as Tar-Related Species for Fuel Gas Cleanup, Energy Fuels. 17 (2003) 329–337. doi:10.1021/ef0201533.
[71] G. Taralas, M.G. Kontominas, Kinetic modelling of VOC catalytic steam pyrolysis for tar abatement phenomena in gasification/pyrolysis technologies, Fuel. 83 (2004) 1235–1245. doi:10.1016/j.fuel.2003.11.010.
[72] G. Lammers, A. a. C.M. Beenackers, J. Corella, Catalytic Tar Removal from Biomass Producer Gas with Secondary Air, in: Dev. Thermochem. Biomass Convers., Springer, Dordrecht, 1997: pp. 1179–1193. doi:10.1007/978-94-009-1559-6_95.
[73] H. Kobayashi, M. Yamaguchi, T. Ito, Ab initio MO study on adsorption of a hydrogen molecule onto magnesium oxide (100) surface, J. Phys. Chem. 94 (1990) 7206–7213. doi:10.1021/j100381a047.
[74] H. Hattori, Heterogeneous Basic Catalysis, Chem. Rev. 95 (1995) 537–558. doi:10.1021/cr00035a005.
[75] C.P.B. Quitete, M.M.V.M. Souza, Application of Brazilian dolomites and mixed oxides as catalysts in tar removal system, Appl. Catal. Gen. 536 (2017) 1–8. doi:10.1016/j.apcata.2017.02.014.
[76] S. Nakamura, S. Kitano, K. Yoshikawa, Biomass gasification process with the tar removal technologies utilizing bio-oil scrubber and char bed, Appl. Energy. 170 (2016) 186–192. doi:10.1016/j.apenergy.2016.02.113.
[77] P. Brandt, E. Larsen, U. Henriksen, High Tar Reduction in a Two-Stage Gasifier, Energy Fuels. 14 (2000) 816–819. doi:10.1021/ef990182m.
[78] Y. Shao, D. Meng, C.C. Xu, F. Preto, J. Zhu, Ash Deposition in Air-Blown Gasification of Peat and Woody Biomass in a Fluidized-Bed Gasifier, Energy Fuels. (2018). doi:10.1021/acs.energyfuels.8b00158.
[79] S. Rapagnà, K. Gallucci, P.U. Foscolo, Olivine, dolomite and ceramic filters in one vessel to produce clean gas from biomass, Waste Manag. 71 (2018) 792–800. doi:10.1016/j.wasman.2017.07.038.
[80] Y. Tian, X. Zhou, S. Lin, X. Ji, J. Bai, M. Xu, Syngas production from air-steam gasification of biomass with natural catalysts, Sci. Total Environ. 645 (2018) 518–523. doi:10.1016/j.scitotenv.2018.07.071.
[81] M. Jeremiáš, M. Pohořelý, K. Svoboda, S. Skoblia, Z. Beňo, M. Šyc, CO2 gasification of biomass: The effect of lime concentration in a fluidised bed, Appl. Energy. 217 (2018) 361–368. doi:10.1016/j.apenergy.2018.02.151.
[82] S. Kern, C. Pfeifer, H. Hofbauer, Reactivity tests of the water–gas shift reaction on fresh and used fluidized bed materials from industrial DFB biomass gasifiers, Biomass Bioenergy. 55 (2013) 227–233. doi:10.1016/j.biombioe.2013.02.001.
[83] F. Kirnbauer, V. Wilk, H. Kitzler, S. Kern, H. Hofbauer, The positive effects of bed material coating on tar reduction in a dual fluidized bed gasifier, Fuel. 95 (2012) 553–562. doi:10.1016/j.fuel.2011.10.066.
[84] F. Kirnbauer, H. Hofbauer, Investigations on Bed Material Changes in a Dual Fluidized Bed Steam Gasification Plant in Güssing, Austria, Energy Fuels. 25 (2011) 3793–3798. doi:10.1021/ef200746c.
[85] F. Kirnbauer, H. Hofbauer, The mechanism of bed material coating in dual fluidized bed biomass steam gasification plants and its impact on plant optimization, Powder Technol. 245 (2013) 94–104.
[86] M. Kuba, F. Havlik, F. Kirnbauer, H. Hofbauer, Influence of bed material coatings on the water-gas-shift reaction and steam reforming of toluene as tar model compound of biomass gasification, Biomass Bioenergy. 89 (2016) 40–49. doi:10.1016/j.biombioe.2015.11.029.

[87] M. Kuba, H. He, F. Kirnbauer, D. Boström, M. Öhman, H. Hofbauer, Deposit build-up and ash behavior in dual fluid bed steam gasification of logging residues in an industrial power plant, Fuel Process. Technol. 139 (2015) 33–41. doi:10.1016/j.fuproc.2015.08.017.
[88] M. Kuba, H. He, F. Kirnbauer, N. Skoglund, D. Boström, M. Öhman, H. Hofbauer, Mechanism of Layer Formation on Olivine Bed Particles in Industrial-Scale Dual Fluid Bed Gasification of Wood, Energy Fuels. 30 (2016) 7410–7418. doi:10.1021/acs.energyfuels.6b01522.
[89] L. Coll, EQTEC GASIFIER TECHNOLOGY, in: Hamburg, Germany, 2014.
[90] J. Carignan, P. Hild, G. Mevelle, J. Morel, D. Yeghicheyan, Routine analyses of trace elements in geological samples using flow injection and low pressure on-line liquid chromatography and ICP-MS: A study of geochemichal reference materials BR, DR-N, UB-N, AN-G and GH, Geostand. Geoanalytical Res. 25 (2001) 187–198.
[91] R.N. Olcese, M. Bettahar, D. Petitjean, B. Malaman, F. Giovanella, A. Dufour, Gas-phase hydrodeoxygenation of guaiacol over Fe/SiO2 catalyst, Appl. Catal. B Environ. 115–116 (2012) 63–73. doi:10.1016/j.apcatb.2011.12.005.
[92] J. Kaknics, R. Michel, J. Poirier, E. de Bilbao, Experimental Study and Thermodynamic Modelling of High Temperature Interactions Between Molten Miscanthus Ashes and Bed Particles in Fluidized Bed Reactors, Waste Biomass Valorization. 8 (2017) 2771–2790. doi:10.1007/s12649-017-9828-x.
[93] R. Michel, J. Kaknics, E. de Bilbao, J. Poirier, The mechanism of agglomeration of the refractory materials in a fluidized-bed reactor, Ceram. Int. 42 (2016) 2570–2581. doi:10.1016/j.ceramint.2015.10.060.
[94] N. Alarcón, X. García, M. Centeno, P. Ruiz, A. Gordon, Catalytic cooperation at the interface of physical mixtures of CaO and MgO catalysts during steam gasification of naphthalene, Surf. Interface Anal. 31 (n.d.) 1031–1041. doi:10.1002/sia.1137.
[95] V. Derycke, M. Kongolo, M. Benzaazoua, M. Mallet, O. Barrès, P. De Donato, B. Bussière, R. Mermillod-Blondin, Surface chemical characterization of different pyrite size fractions for flotation purposes, Int. J. Miner. Process. 118 (2013) 1–14. doi:10.1016/j.minpro.2012.10.004.
[96] A.P.E. York, T. Xiao, M.L.H. Green, J.B. Claridge, Methane Oxyforming for Synthesis Gas Production, Catal. Rev. 49 (2007) 511–560. doi:10.1080/01614940701583315.
[97] J.C. Lavalley, Infrared spectrometric studies of the surface basicity of metal oxides and zeolites using adsorbed probe molecules, Catal. Today. 27 (1996) 377–401. doi:10.1016/0920-5861(95)00161-1.
[98] V.A. Rigo, C.O. Metin, Q.P. Nguyen, C.R. Miranda, Hydrocarbon Adsorption on Carbonate Mineral Surfaces: A First-Principles Study with van der Waals Interactions, J. Phys. Chem. C. 116 (2012) 24538–24548. doi:10.1021/jp306040n.
[99] H. Itoh, S. Utamapanya, J.V. Stark, K.J. Klabunde, J.R. Schlup, Nanoscale Metal Oxide Particles as Chemical Reagents. Intrinsic Effects of Particle Size on Hydroxyl Content and on Reactivity and Acid/Base Properties of Ultrafine Magnesium Oxide, Chem. Mater. 5 (1993) 71–77. doi:10.1021/cm00025a015.
[100] R.G. Pearson, Acids and Bases, Science. 151 (1966) 172–177. doi:10.1126/science.151.3707.172.
[101] R.G. Pearson, Absolute electronegativity and hardness: application to inorganic chemistry, Inorg. Chem. 27 (1988) 734–740. doi:10.1021/ic00277a030.
[102] W.C. Conner, J.L. Falconer, Spillover in Heterogeneous Catalysis, Chem. Rev. 95 (1995) 759–788. doi:10.1021/cr00035a014.
[103] R. Philipp, K. Omata, A. Aoki, K. Fujimoto, On the active site of MgO/CaO mixed oxide for oxidative coupling of methane, J. Catal. 134 (1992) 422–433. doi:10.1016/0021-9517(92)90332-C.
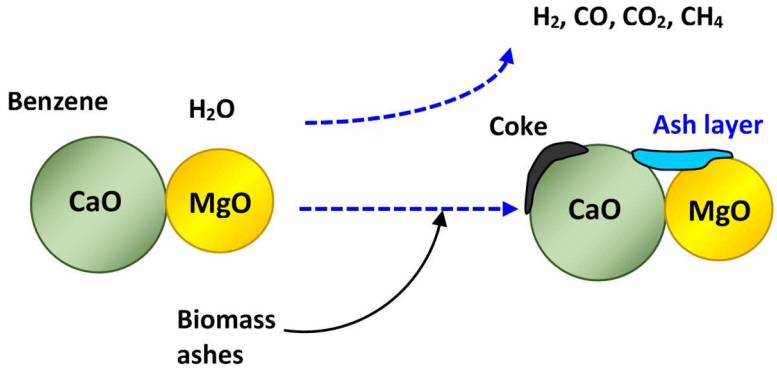
Graphical abstract